Review | Open Access

Energy Materials

Lee *et al. Energy Mater.* **2026**, *6*, 600087 **DOI:**10.20517/energymater.2026.95

Beyond inorganic cathodes: organic and open-framework electrode materials for aqueous manganese-ion batteries

Hyeongseok Lee, Jiwoong Yang, Jeonghun Kim, Munseok S. Chae*

Keywords:
Organic electrode materials, aqueous batteries, hybrid batteries, manganese batteries

Citation: Lee, H.; Yang, J.; Kim, J.; Chae, M. S. Beyond inorganic cathodes: organic and open-framework electrode materials for aqueous manganese-ion batteries. *Energy Mater.* **2026**, *6*, 600087. https://dx.doi.org/10.20517/energymater.2026.95

Received: 28 Apr 2026
First Decision: 5 Jun 2026
Revised: 7 Jul 2026
Accepted: 16 Jul 2026
Published: 30 Jul 2026

Academic Editor: Yuping Wu
Copy Editor: Ping Zhang
Production Editor: Ping Zhang

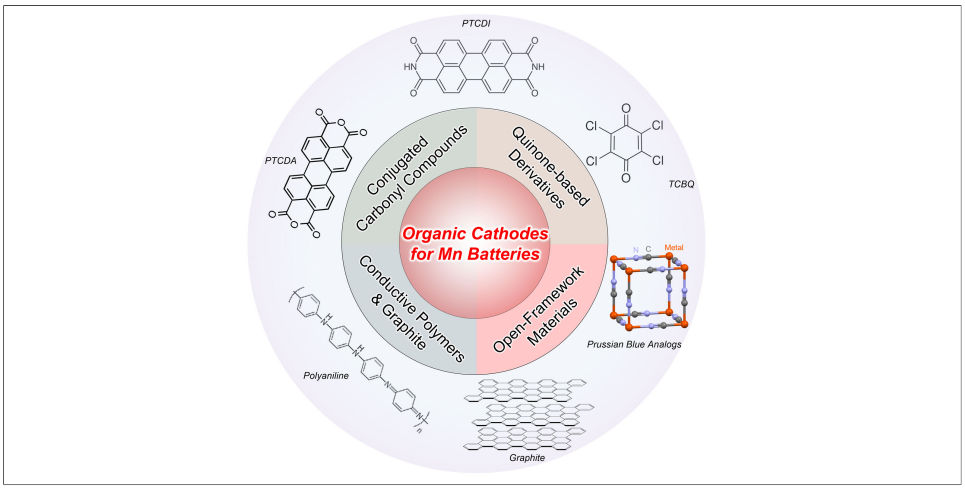

Abstract

Manganese-ion batteries (MIBs) have emerged as compelling candidates for grid-scale energy storage systems, offering superior safety, cost-effectiveness, and competitive electrochemical properties compared to conventional lithium-ion batteries. Despite their potential, the practical deployment of MIBs is significantly hindered by the severe structural degradation of traditional inorganic cathode materials. This degradation is primarily attributed to the strong electrostatic interactions between Mn^{2+} ions and the associated structural distortion. This review systematically elucidates the strategic design principles and electrode materials for manganese-based systems, positioning organic cathode materials as transformative alternatives to overcome these persistent limitations. Specifically, we evaluate the performance of various organic cathode materials, including conjugated carbonyl compounds and quinone derivatives, with an emphasis on materials that provide low-strain pathways through precise molecular-level engineering. Furthermore, we discuss the pivotal roles of conducting polymers and open-framework Prussian Blue analogs in ensuring stable power output and rapid ion diffusion. Particular focus is placed on high-entropy stabilization strategies, which serve as a key mechanism for enhancing long-term cycling stability. Additionally, this review covers graphite-based dual-ion systems that effectively transcend the operational voltage limitations of

Department of Nanotechnology Engineering, Pukyong National University, Busan 48513, Republic of Korea.

***Correspondence to:** Prof. Munseok S. Chae, Department of Nanotechnology Engineering, Pukyong National University, Busan 48513, Republic of Korea. E-mail: mschae@pknu.ac.kr

conventional MIBs. Finally, we identify critical technical bottlenecks, including active material dissolution, interfacial resistance, and the hydrogen evolution reaction at the Mn metal anode, while providing strategic insights for future research directions.

INTRODUCTION

Amid the escalating global climate crisis and the imperative to decouple from fossil fuel dependency, the transition toward renewable energy systems has emerged as an indispensable global mandate rather than a mere option. However, to overcome the inherent intermittency of renewable energy sources such as solar and wind power, the development of grid-scale energy storage systems (ESS) must unequivocally be supported[1]. Currently, lithium-ion batteries (LIBs) dominate the market due to their high energy density[2]; nevertheless, the limited reserves and price volatility of critical resources like lithium (Li), nickel (Ni), and cobalt (Co) pose significant constraints on their large-scale deployment[3]. Furthermore, the risks of fire and explosion, stemming from flammable organic electrolytes and the high reactivity of lithium metal, remain fatal vulnerabilities in the deployment of ESS[4,5].

To address these safety and resource constraints, aqueous batteries utilizing water-based electrolytes have emerged as a compelling alternative, offering both economic feasibility and non-flammability[6-8]. In particular, amidst growing interest in multivalent-ion batteries capable of multi-electron redox reactions, manganese (Mn) possesses unrivaled competitiveness among various metal anode candidates, including alkali metals (Li, K) and transition metals (Zn, Co, Ni)[9-11]. As compared in Figure 1A, although alkali metals like Li and K offer high theoretical capacities (3,861 and 685 mAh/g, respectively) and exceptionally low potentials [-3.05 and -2.93 V *vs.* standard hydrogen electrode (SHE)], their extreme reactivity in water and high costs (20 and 13 USD/kg) limit their practical use in safe aqueous systems[9]. Meanwhile, typical transition metals used in conventional cathodes, such as Co and Ni, suffer from severe resource scarcity (25 and 80 ppm abundance) and high costs (30 and 20 USD/kg)[10]. Zinc (Zn) is inexpensive (2 USD/kg) and highly stable in water, but its high reduction potential (-0.76 V *vs.* SHE) and low capacity (820 mAh/g) restrict the overall cell voltage and energy density[11]. In this context, Mn represents an optimal trade-off; it combines low cost (2 USD/kg), high crustal abundance (950 ppm), a low reduction potential (-1.19 V *vs.* SHE), and a high capacity (976 mAh/g), making it highly advantageous for high-voltage, cost-effective aqueous batteries[12,13].

Recent research has focused on electrolyte optimization strategies to enhance the reversibility of these Mn metal anodes. Configurations that utilize such metallic components and rely on the electrochemical plating and stripping of Mn^{2+} ions on the anode surface are specifically designated as manganese metal batteries. Moving beyond initial $MnSO_4$- and $MnCl_2$-based systems, advanced salt systems such as $Mn(ClO_4)_2$ and $Mn(TFSI)_2$ are being introduced to suppress the hydrogen evolution reaction (HER)[14-17]. Meanwhile, interfacial engineering strategies utilizing additives like sucrose and glycine have achieved remarkable breakthroughs. Furthermore, the exploration of non-aqueous and hybrid electrolytes incorporating acetonitrile (AcN)[18], dimethyl sulfoxide (DMSO)[19], ethylene carbonate (EC)[14], and ethylene glycol (EG)[20] further expands the operating voltage window of Mn batteries, thereby elevating the feasibility of their practical application.

Despite advancements in electrolyte and anode technologies, the development of cathode materials capable of stably accommodating multivalent Mn^{2+} ions remains a formidable hurdle. Conventional inorganic cathode materials, such as Vanadium-based oxides[20-23], suffer from rapid structural degradation due to strong electrostatic interactions or Jahn-Teller distortion. To overcome such physical rigidity, this review proposes organic cathode materials (OCMs) as an innovative alternative[24]. As indicated by the comparative

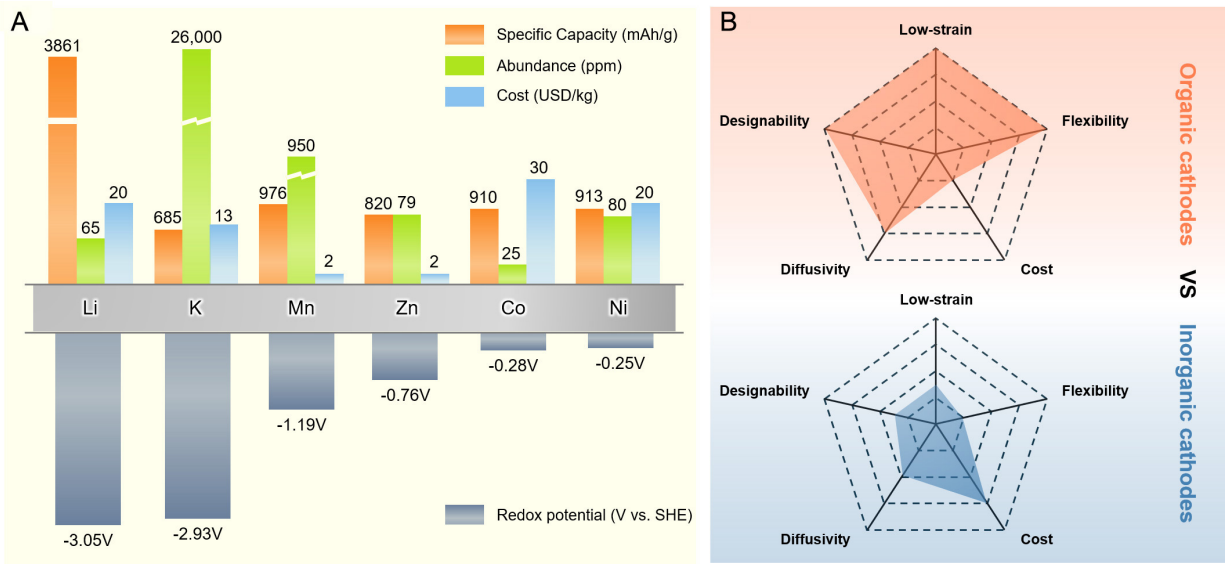

Figure 1. (A) Comparison of elemental abundance and fundamental characteristics of representative elements used in rechargeable batteries; (B) Schematic comparison of key performance parameters between organic and inorganic cathodes. SHE: Standard hydrogen electrode.

metrics in Figure 1B, unlike inorganic lattices, organic materials enable precise molecular-level design. They also provide low-strain reaction pathways that flexibly accommodate the stress generated during ion insertion, owing to their intrinsic structural flexibility, thereby alleviating the structural instability typically observed in inorganic cathodes. Nevertheless, this research field remains in its early stage, and only a limited number of organic electrode materials have been reported so far.

Among the reported materials, conjugated carbonyl compounds such as perylene-3,4,9,10-tetracarboxylic dianhydride (PTCDA)[25,26] and perylene-3,4,9,10-tetracarboxylic diimide (PTCDI)[27-29] exhibit enhanced electrical conductivity and structural robustness owing to their strong π-π stacking interactions. Quinone derivatives, including tetrachloro-1,4-benzoquinone (TCBQ,4-Cl-BQ)[11,29], enable precise tuning of the operating voltage through functional group engineering. In addition, conductive polymers such as Polyaniline (PANI)[30] and open-framework materials like Prussian Blue analogs provide spacious ion-transport channels that facilitate the rapid diffusion of Mn^{2+} ions.

In this review, we systematically survey recent progress in manganese-ion battery systems, spanning electrolyte optimization strategies for stabilizing Mn metal anodes and the structure-performance relationships of organic cathode materials. Particular emphasis is placed on understanding the underlying reaction mechanisms of organic electrodes and identifying key molecular design parameters for next-generation materials. Through this comprehensive perspective, we aim to establish design principles that can overcome the intrinsic limitations of conventional inorganic cathodes and enable high-voltage, safe manganese-based energy storage systems.

Organic and open-framework electrode materials: design principles and mechanisms

Manganese-ion batteries, which represent electrochemical systems in which manganese ions primarily participate in redox reactions, have to date mostly employed cathode materials based on inorganic compounds. Among them, vanadium-based materials have been extensively studied owing to their favorable redox chemistry and relatively open frameworks[31-33]. However, these materials frequently suffer from structural degradation and vanadium dissolution during electrochemical cycling, which limits their long-term stability.

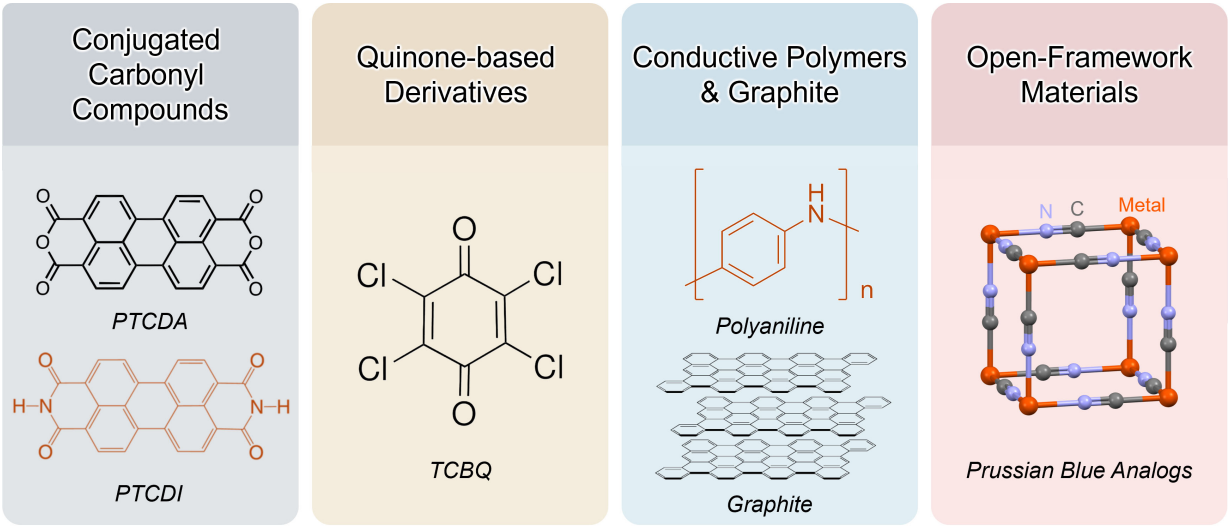

Figure 2. Schematic overview of organic cathode materials for manganese-ion batteries. PTCDA: Perylene-3,4,9,10-tetracarboxylic dianhydride; PTCDI: perylene-3,4,9,10-tetracarboxylic diimide.

In contrast, organic electrode materials offer unique advantages because their electrochemical properties can be precisely tailored through molecular-level design. Despite these promising features, the exploration of organic materials for manganese-ion batteries remains limited due to the early stage of research in this field. The reported systems can generally be classified into several categories [Figure 2], including conjugated carbonyl compounds, quinone derivatives, conductive polymers, open-framework materials, and carbon-based anion intercalation hosts. In the following sections, we critically review representative examples from each category and discuss their underlying charge-storage mechanisms and design principles.

CONJUGATED CARBONYL COMPOUNDS

PTCDA

The Mn-ion storage mechanism in PTCDA is governed by the reversible coordination between its internal carbonyl groups (C=O) and Mn^{2+} ions[25,26]. As depicted in Figure 3A and B, the C=O functional groups undergo a transition to C-O-Mn during the discharge process, effectively storing charge. Distinct from inorganic hosts with fixed lattice structures, these redox-active organic materials offer superior molecular-level designability, facilitating the development of optimized electrodes for multivalent-ion storage. Structurally, PTCDA features a robust π-π stacking configuration that ensures both electronic conductivity and structural integrity. As shown in Figure 3C, this stacking provides expansive diffusion channels for Mn^{2+} ions, maintaining a stable interlayer distance of approximately 3.7 Å. Theoretical calculations suggest that the PTCDA framework exhibits negligible volumetric expansion during Mn^{2+} insertion, as multiple coordination sites stabilize the intercalated ions through electrostatic interactions. This inherent structural flexibility is pivotal to overcoming the limitations of conventional inorganic cathodes, such as V_2O_5 and MnO_2, which often suffer from severe structural degradation induced by Jahn-Teller distortion and strong electrostatic repulsion during multivalent-ion insertion. Consequently, PTCDA offers a low-strain pathway that elastically accommodates mechanical stress, thereby fundamentally resolving chronic structural instability issues. Electrochemical performance evaluations further validate the high reversibility of the PTCDA electrode. Cyclic voltammetry (CV) analysis at a scan rate of 0.3 mV/s [Figure 3D] reveals well-defined and symmetrical redox peak pairs, indicating that the stepwise coordination remains highly reversible even under accelerated kinetics[26]. Furthermore, the symmetry of the peaks suggests minimal interfacial resistance during insertion and extraction. The galvanostatic charge-discharge (GCD) profiles at various current densities exhibit nearly overlapping curves from the 1st to the 5th cycle [Figure 3E], yielding a stable

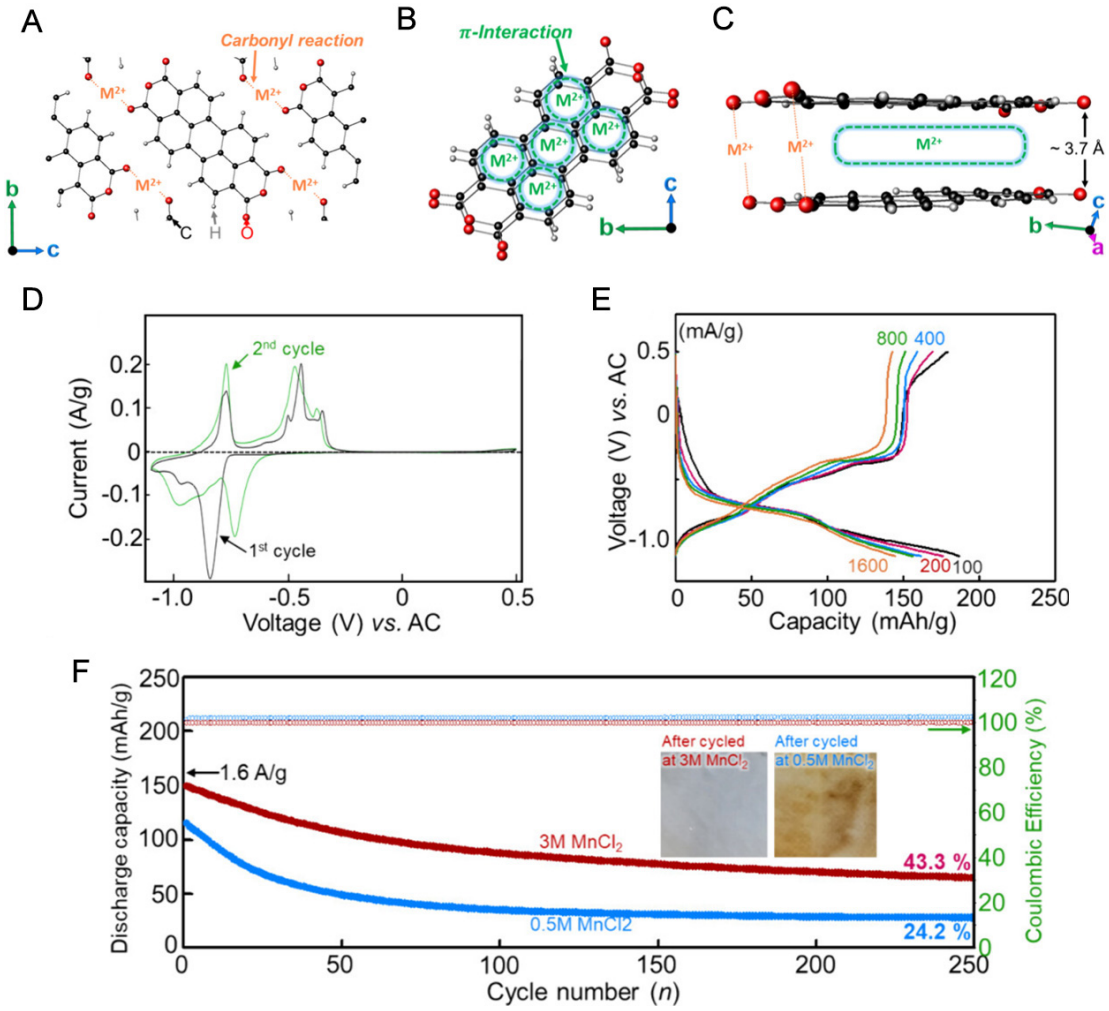

Figure 3. Structural analysis and electrochemical characterization of PTCDA electrodes. (A-C) Schematic illustrations of the PTCDA crystallographic structure, highlighting the active carbonyl reaction sites and π-interaction regions within the bc-plane and ab-plane configurations; (D) CV profile recorded at a scan rate of 0.3 mV/s. (E) GCD curves obtained at various current densities; (F) Long-term cycling stability and coulombic efficiency evaluated at a specific current of 1.6 A/g. Reprinted with permission from Ref.[26]. Copyright © 2024 American Chemical Society. CV: Cyclic voltammetry; PTCDA: perylene-3,4,9,10-tetracarboxylic dianhydride; GCD: galvanostatic charge-discharge.

reversible capacity of approximately 170 mAh/g. This exceptional overlap indicates minimal irreversible transformation of the host lattice during Mn^{2+} ion insertion and extraction, which stands in stark contrast to the significant initial capacity loss typically observed in inorganic cathode counterparts. Complementing these findings, long-term cycling tests conducted at a current density of 1.6 A/g [Figure 3F] demonstrate remarkable stability, with the initial capacity being effectively maintained over 250 cycles. Furthermore, the consistently high Coulombic efficiency observed throughout the process underscores the successful suppression of parasitic reactions, such as electrode dissolution or electrolyte decomposition[26].

In summary, PTCDA successfully addresses the structural vulnerabilities of inorganic cathode materials through its flexible organic framework, presenting significant potential as a reliable electrode for next-generation aqueous Mn-ion batteries.

PTCDI

PTCDI represents a prominent organic electrode material that shares a perylene framework with PTCDA while offering superior chemical stability in aqueous environments due to its imide functional groups. The

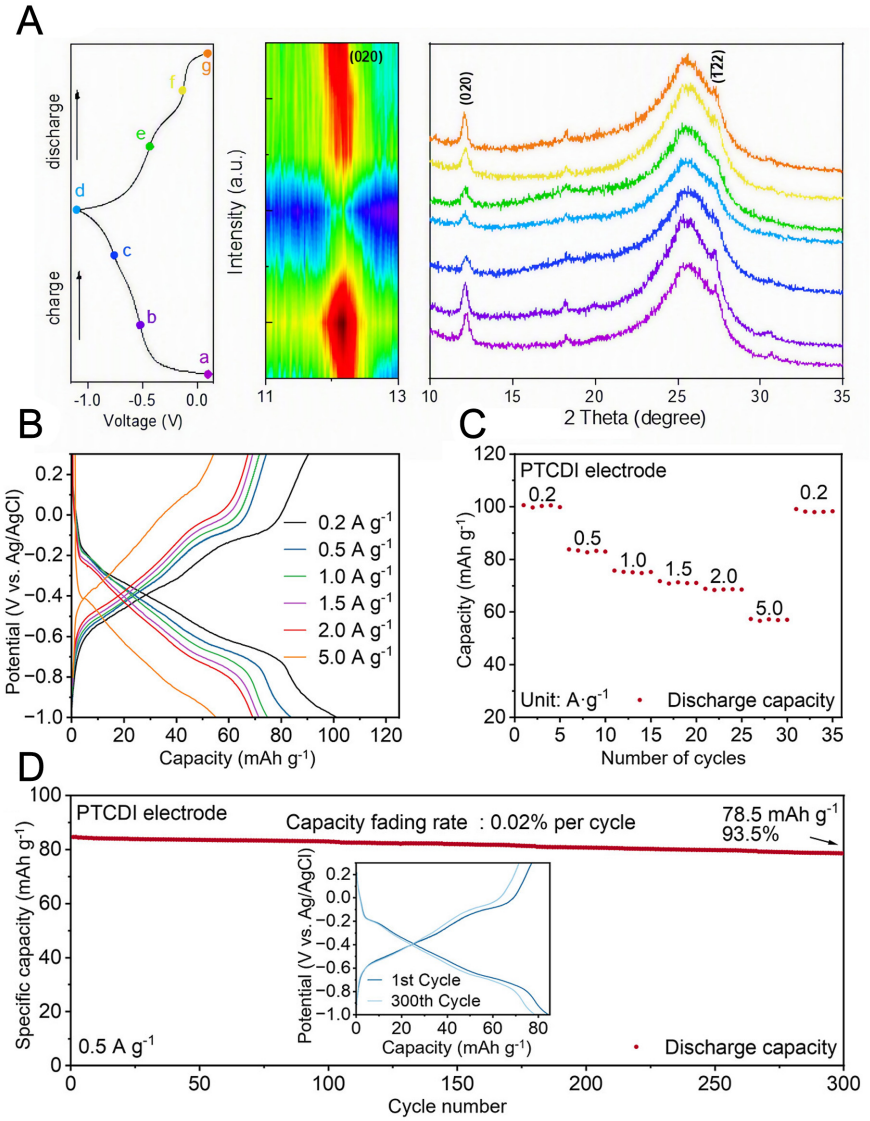

Figure 4. Electrochemical characterization and structural evolution of the PTCDI electrode. (A) GCD curve and corresponding *ex-situ* XRD patterns recorded at selected states to elucidate the energy storage mechanism. (A) Reprinted with permission from Ref.[29]. Copyright © 2025 Wiley; (B) GCD profiles and (C) Rate capability of the PTCDI electrode obtained at various current densities. (D) Long-term cycling performance and stability of the PTCDI electrode at a specific current of 0.5 A/g. (B-D) Reprinted with permission from Ref.[27]. Copyright © 2025 American Chemical Society. XRD: X-ray diffraction; PTCDI: perylene-3,4,9,10-tetracarboxylic diimide; GCD: galvanostatic charge-discharge.

ex-situ X-ray diffraction (XRD) analysis presented in Figure 4A underscores the material's exceptional structural reversibility; although the (020) and (122) diffraction peaks undergo subtle shifts during Mn^{2+} ion intercalation and de-intercalation, they return precisely to their pristine positions upon recharging. This robust stability originates from strong intermolecular π-π interactions and the flexibility of the organic backbone, which collectively accommodate mechanical strain without triggering a lattice collapse[29].

Regarding kinetic performance, the PTCDI electrode displays exceptional rate capability [Figure 4B][27]. In particular, it maintains stable discharge capacities from 100.5 to 57.3 mAh/g across a broad range of current densities from 0.2 to 5.0 A/g. These performance metrics represent a capacity utilization of approximately 73.6% to 41.9% relative to the theoretical limit of 136.6 mAh/g, assuming a two-electron redox process at the carbonyl sites. Furthermore, as shown in Figure 4C, the electrode exhibits remarkable resilience, showing

negligible capacity degradation when the current density is restored to 0.2 A/g following high-rate testing. GCD profiles reveal well-defined voltage plateaus at approximately -0.38 V and -0.67 V (*vs.* Ag/AgCl) during the discharge phase, and -0.11 V and -0.4 V (*vs.* Ag/AgCl) during the charge phase. A hallmark of PTCDI is its unprecedented cycling stability within Mn-ion eutectic electrolyte systems[27]. When tested at a current density of 0.5 A/g, the electrode retains approximately 93.5% of its initial capacity (78.5 mAh/g) after 300 cycles [Figure 4D]. This corresponds to an incredibly low-capacity fade of just 0.02% per cycle, a result that stands in stark contrast to the 68.1% retention observed in conventional $Mn(ClO_4)_2$ electrolytes lacking acetamide. This significant enhancement is primarily driven by the eutectic electrolyte's ability to suppress active-material dissolution and parasitic side reactions associated with free water molecules - two major challenges for organic battery chemistry.

Analogous to PTCDA, PTCDI represents a key member of the conjugated carbonyl compound family, utilizing its internal carbonyl (C=O) groups as active redox centers. Both materials benefit from high molecular designability and intrinsic structural flexibility, which allow them to effectively mitigate structural degradation typically induced by strong electrostatic interactions or Jahn-Teller distortion in inorganic transition-metal oxide cathodes[34]. Consequently, conjugated carbonyl compounds such as PTCDA and PTCDI provide low-strain reaction pathways that elastically accommodate the mechanical stress associated with multivalent ion insertion, highlighting their strong potential as cathode materials for high-performance aqueous Mn-ion batteries.

PTCDI incorporates imide moieties that impart exceptional chemical durability, effectively circumventing electrode dissolution and preserving the structural framework during prolonged electrochemical operation, whereas PTCDA is intrinsically susceptible to hydrolysis in aqueous electrolytes owing to its anhydride functional groups. Furthermore, the substitution of oxygen with nitrogen fundamentally modulates the local electron density, driving highly stable and reversible redox kinetics. As elucidated in the work of Liebl *et al.*, the N-H bonds within the imide groups facilitate robust intermolecular hydrogen-bonding networks with adjacent molecules[35]. This hydrogen bonding significantly reinforces the host lattice, yielding outstanding structural durability and low-strain characteristics that are critical for the stable accommodation of Mn^{2+} ions. The macroscopic impact of these molecular-level disparities is unambiguously demonstrated in the long-term cycling performance; comparing Figure 3F and Figure 4D confirms that PTCDI achieves a substantially enhanced cycle life and superior capacity retention relative to the hydrolysis-prone PTCDA.

Importantly, conjugated carbonyl compounds often exhibit dual charge-storage characteristics. Charge storage can occur through enolate formation at carbonyl sites as well as through cation interactions with the π-electron system of adjacent aromatic rings. This indicates that maximizing cation-storage capability does not simply rely on increasing the number of carbonyl groups; rather, the presence of aromatic rings and their stacking configuration play a crucial role in governing ion-storage behavior. Therefore, rational molecular engineering of carbonyl groups and aromatic frameworks, including their numbers, spatial arrangements, and stacking configurations, represents an effective strategy for designing next-generation conjugated carbonyl cathodes with enhanced electrochemical performance.

QUINONE-BASED DERIVATIVES (TCBQ, 4-CL-BQ)

Quinone derivatives represent a highly promising class of cathode candidates for energy storage systems, primarily due to their significant molecular variability, which allows for the optimization of electrochemical properties by modulating the chemical environment near the active sites. Among these, TCBQ (or 4-Cl-BQ) features a benzoquinone skeleton coupled with four strong electron-withdrawing chlorine (-Cl) atoms[11,29]. This structural configuration effectively lowers the lowest unoccupied molecular orbital (LUMO) level

compared to unsubstituted quinones, serving as a critical design principle for significantly elevating the reduction potential and, consequently, the operating voltage.

According to the study by Bi *et al.*[11], the TCBQ cathode facilitates energy storage through a reversible enolization mechanism, where carbonyl groups react with Mn ions. Through this process, TCBQ achieves a remarkably high and stable discharge plateau at approximately 1.37 V, providing a superior voltage advantage over conventional inorganic-based manganese battery systems. A key intrinsic strength of such organic cathodes is their structural flexibility, which enables them to effectively accommodate the physical stress induced during repetitive ion insertion. This flexibility allows organic hosts to overcome the limitations of common inorganic electrodes, which are often susceptible to mechanical degradation caused by reliance on rigid ion-diffusion pathways, thereby maintaining high reversibility.

The superior characteristics of this organic cathode were further validated by evaluating a full-cell system. Figure 5A provides a schematic illustration of the designed aqueous Mn-ion full cell, utilizing a PTCDI anode and a TCBQ cathode[29]. The reaction kinetics of this system were analyzed via CV profiles in Figure 5B, which exhibit sharp and symmetrical redox peaks across a wide range of scan rates from 1.0 to 10.0 mV/s. These profiles indicate that charge transfer at the electrode interface occurs rapidly and efficiently. In the GCD curves shown in Figure 5C, the cell recorded a high specific capacity of approximately 98 mAh/g at a current density of 1.0 A/g while maintaining a stable voltage platform. Furthermore, the rate evaluated in Figure 5D demonstrates exceptional power performance, retaining a significant portion of the initial capacity even under a demanding current density of 10.0 A/g. Most notably, the long-term cycling test presented in Figure 5E confirms outstanding reliability, with negligible capacity loss over 1,000 cycles at 1.0 A/g. This performance highlights the advantages of the structural robustness of organic hosts in long-term operational environments. Despite these excellent properties, small-molecule organic cathodes such as TCBQ face a fundamental challenge regarding their dissolution in aqueous electrolytes. To address this issue, transitioning from conventional salts to acetate (Ac^-)-based electrolytes has emerged as a highly effective strategy. The strong coordination ability of acetate ions fundamentally alters the solvation structure of Mn^{2+} ions, significantly lowering the desolvation energy barrier at the electrode-electrolyte interface[27,29]. This modification not only accelerates the charge-transfer and redox kinetics but also effectively minimizes water activity, thereby suppressing both parasitic side reactions and active material leaching. Consequently, the utilization of acetate-based salt systems enables stable Mn plating/stripping behavior at the anode while robustly protecting the organic framework at the cathode, ultimately delivering a noticeably enhanced capacity retention and prolonged cycling stability[29].

Overall, TCBQ cathodes, characterized by their molecular-level voltage tunability and intrinsic structural flexibility, represent promising candidates for next-generation high-energy and long-life aqueous batteries when combined with advanced electrolyte stabilization strategies. Compared with PTCDA-based systems, TCBQ exhibits a higher operating voltage, which is advantageous for improving the overall energy density of manganese-ion batteries[29]. However, TCBQ inherently has a relatively low capacity due to the limited number of redox-active sites. Addressing this limitation will require rational molecular design strategies, such as reducing molecular weight and increasing the density of redox-active functional groups[36]. Through such molecular engineering approaches, it may be possible to develop organic cathode materials that simultaneously achieve both high operating voltage and high capacity.

CONDUCTIVE POLYMERS (POLYANILINE)

PANI has emerged as a compelling cathode material for Mn-based hybrid batteries, which represent electrochemical systems where auxiliary ions (such as protons) co-intercalate with Mn^{2+} ions to drive synergistic redox chemistry[37]. As a representative conductive polymer featuring a chain-like framework of

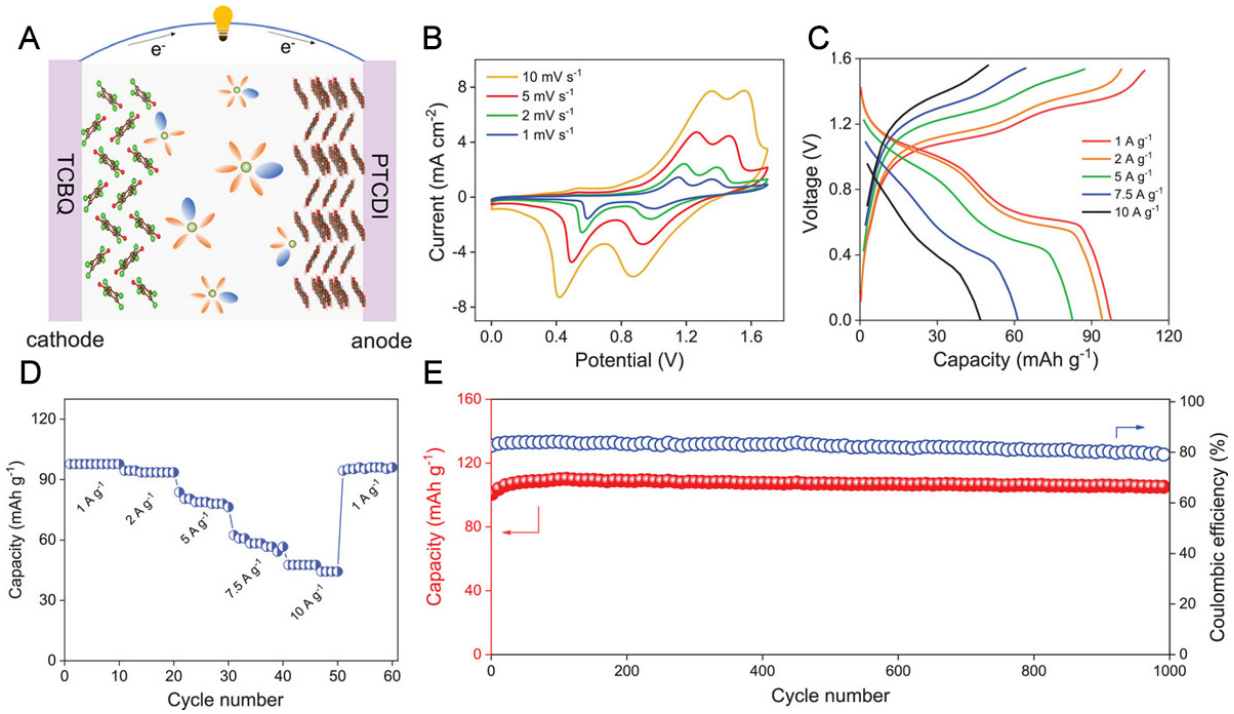

Figure 5. Full-cell performance and electrochemical evaluation of the PTCDI//TCBQ aqueous Mn-ion battery. (A) Schematic illustration of the designed aqueous Mn-ion full cell; (B) CV profiles recorded at various scan rates from 1.0 to 10 mV/s; (C and D) Rate capability and corresponding GCD curves evaluated across a range of current densities; (E) Long-term cycling performance of the full cell at a constant current density of 1.0 A/g. Reprinted with permission from Ref.[29]. Copyright © 2025 Wiley. TCBQ: Tetrachloro-1,4-benzoquinone; CV: cyclic voltammetry; GCD: galvanostatic charge-discharge; PTCDA: perylene-3,4,9,10-tetracarboxylic dianhydride; PTCDI: perylene-3,4,9,10-tetracarboxylic diimide.

alternating benzene rings and amine groups, characterized by a semi-crystalline structure where crystalline and amorphous regions coexist[30]. Simultaneously, it possesses a porous architecture that serves as an efficient pathway for ion transport. This semi-crystalline and porous morphology maximizes internal conductivity, effectively addressing the inherent limitation of low electrical conductivity in inorganic cathode materials and enabling superior electrochemical performance without the addition of separate conductive agents, such as carbon black[30].

To evaluate the electrochemical behavior of the PANI electrode, a CV profile was recorded over the potential range -0.7 V to 0.7 V at a scan rate of 0.1 mV/s [Figure 6A][30]. The resulting profile displays a clear oxidation peak at 0.2 V and distinct reduction peaks at -0.24, 0.08, and 0.18 V. These multiple redox peaks indicate that the storage and removal of Mn^{2+} ions within the PANI framework are highly reversible. GCD profile results [Figure 6B] recorded a specific capacity of approximately 88.3 mAh/g at a current density of 0.25 A/g, where the overall flat potential slope confirming a uniform distribution of redox sites. Notably, the maintenance of this flat slope even at high current densities suggests that the high intrinsic conductivity of PANI minimizes voltage drops (Internal resistance drops, IR drops) during rapid charge/discharge cycles. The rate capability and structural resilience were evaluated using a stepped cycling test [Figure 6C], revealing that capacity almost fully recovered to approximately 91.5 mAh/g when the current density was reduced from 1.0 A/g to 0.25 A/g. This recovery is attributed to the high flexibility and structural elasticity of the organic polymer framework. Long-term reliability was further demonstrated by the cycling performance data [Figure 6D], which showed a high-capacity retention of 67.9% after 1,000 cycles at a current density of 0.5 A/g, alongside a Coulombic efficiency approaching 100%. However, as shown in the Nyquist plot [Figure 6E], a slight increase in resistance was observed after cycling compared to the pristine state, suggesting a gradual decrease in ion mobility resulting from increased interfacial resistance during long-term operation.

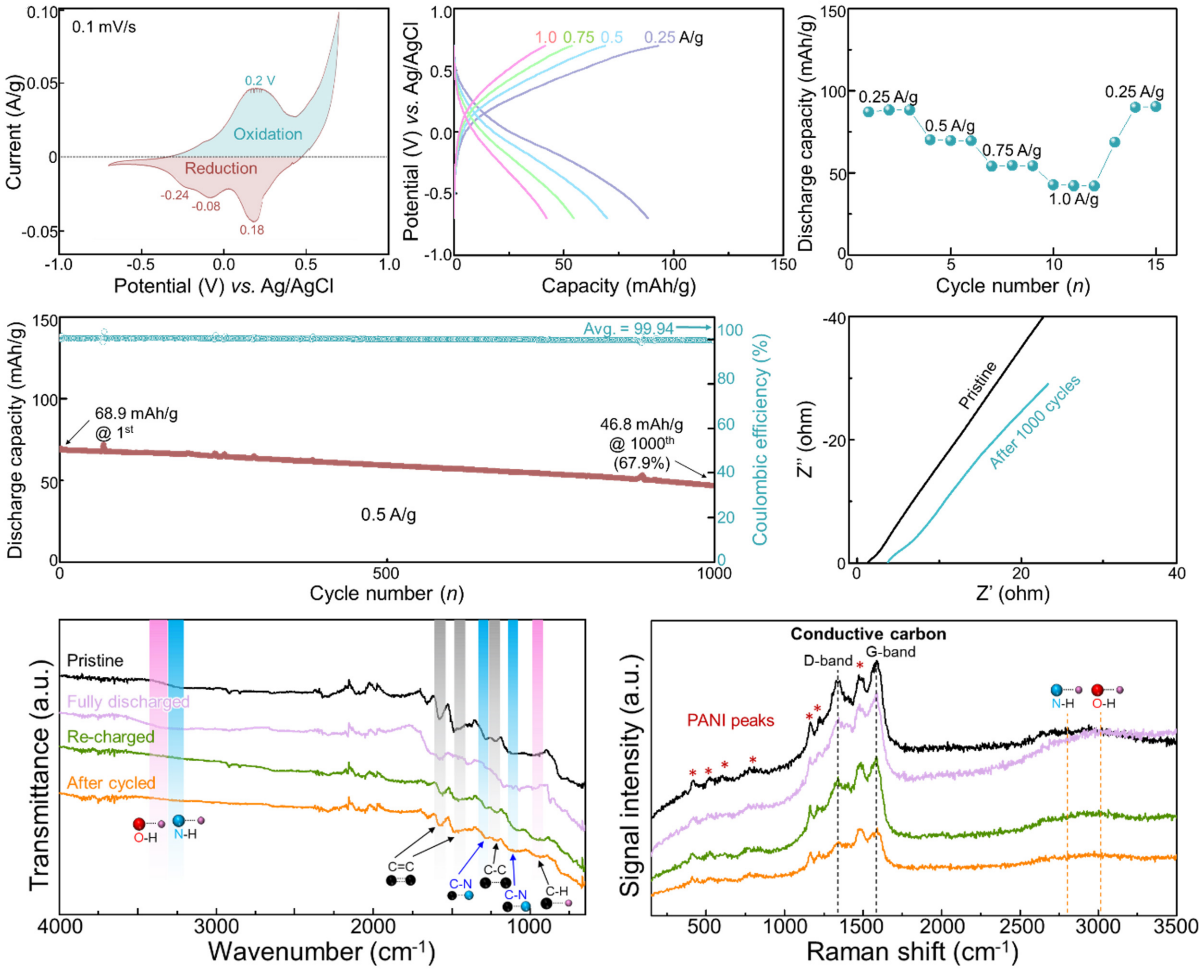

Figure 6. Performance and structural evolution of the PANI electrode. (A) CV curve at 0.1 mV/s; (B) GCD profiles under varying current densities; (C) Rate performance of the PANI electrode; (D) Cycling stability recorded at 0.5 A/g for 1,000 cycles; (E) Nyquist plots before and after 1,000 cycles; (F and G) *Ex-situ* analysis at different electrochemical states showing (F) FTIR and (G) Raman spectra. Reprinted with permission from Ref.[30]. Copyright © 2026 Wiley. PANI: Polyaniline; CV: cyclic voltammetry; GCD: galvanostatic charge-discharge; FTIR: fourier-transform infrared.

Fourier-transform infrared (FTIR) analysis [Figure 6F] was conducted to investigate the structural reversibility of PANI, revealing abrupt signal changes near the C=C, C-C, and C-N bonds during full discharge. These changes are attributed to the co-insertion of water molecules and protonation in the aqueous electrolyte, as evidenced in the 3,405-3,200 cm^{-1} region. The restoration of these bonds to their pristine state upon recharging highlights the exceptional structural flexibility of PANI, while the minimal overall changes after extended cycling confirm its robust structural durability. Raman spectral analysis [Figure 6G] further confirmed that the intrinsic PANI signals were well-maintained, suggesting that the polymer framework remains stable without decomposition over long-term cycling. Specifically, the clear observation of the characteristic D-band (1,338 cm^{-1}) and G-band (1,580 cm^{-1}) of conductive polymers, without significant shifts in peak position or shape after cycling, supports the structural stability of the conductive carbon network. Furthermore, the reversible behavior of the NH (2,796.9 cm^{-1}) and OH (3,030.9 cm^{-1}) bond intensities in the FTIR spectra - which significantly increase during discharge and decrease upon charging - provides definitive evidence of high reversibility[30]. This phenomenon elucidates the mechanism where water molecules enter the electrode due to the simultaneous insertion of manganese ions and protons, resulting in the observed OH signal.

Consequently, the PANI electrode demonstrates stable long-term operation owing to its high reversibility and intrinsic structural flexibility, highlighting its strong potential as a cathode material for next-generation aqueous manganese-ion batteries. More broadly, conductive polymers have been widely recognized as capable charge-storage hosts in battery systems. In particular, the electrochemical performance of PANI-based electrodes can be significantly influenced by structural modifications such as anion substitution and control of the degree of polymerization. Rational tuning of these parameters may provide an effective strategy for optimizing ion-storage behavior and improving overall electrochemical performance. Therefore, further studies focusing on the molecular engineering of conductive polymers will be essential for advancing their practical application in manganese-based energy storage systems.

OPEN-FRAMEWORK MATERIALS (PRUSSIAN BLUE ANALOGS)

Recently, within the field of cathode materials for next-generation secondary batteries, Prussian Blue Analogs (PBAs) have attracted significant research interest. These materials are a subclass of metal-organic frameworks (MOFs) that feature an ordered interconnecting metal architecture. PBAs are characterized by an open 3D framework that provides distinct structural advantages over conventional layered metal oxides or polyanionic compounds. Specifically, the PBA lattice possesses large interstitial sites with a diameter of approximately 4.6 Å[38]. This feature effectively mitigates the strong electrostatic repulsion and high diffusion resistance typically encountered during the intercalation of divalent ions with large hydrated radii such as Mn^{2+}. This structural robustness is pivotal in minimizing lattice strain during repetitive ion insertion and extraction, thereby ensuring superior long-term stability. Generally, PBAs follow the chemical formula $A_xM[Fe(CN)_6]_{y\cdot 1-y}\cdot nH_2O$, where A represents an alkali cation, and M denotes a transition metal[39]. The structural tunability is afforded by the ability to selectively incorporate various transition metals such as Mn, Co, Ni, and Cu into the M-sites. This provides a pathway for performance optimization that is difficult to achieve in purely inorganic oxides. Furthermore, their accessibility through simple co-precipitation methods enhances their potential for industrial-scale application. Recently, the integration of high-entropy (HE) design strategies into PBAs has emerged as a promising approach to maximize electrochemical performance. For instance, studies by He and colleagues demonstrated that High-Entropy PBAs (HEPBAs) applied in sodium-ion batteries could maintain exceptional ultra-long-life characteristics over 10,000 cycles[40].

The Mn-HEPBA structure comprises Mn, Fe, Ni, Co, and Cu. This framework stably accommodates Mn^{2+} ions within its interstitial voids. XRD Rietveld refinement confirms that the material forms a single-phase cubic structure in the *Fm3m* space group with a lattice constant of a = 10.36 Angstroms[41]. The absence of impurity peaks underscores the high phase purity of the synthesized sample. Morphological analysis via Scanning electron microscopy (SEM) and Transmission electron microscopy (TEM) reveals uniform cubic nanostructures approximately 500 nm in size[41]. Furthermore, the well-defined diffraction rings in the selected area electron diffraction (SAED) pattern in correspond to the (220), (222), (400), and (420) planes. This corroborates the formation of a face-centered cubic (FCC) structure with excellent nanoscale crystallinity. Electrochemical characterization reveals that Mn-HEPBA exhibits a charge storage behavior distinct from that of conventional Mn-PBA. A comparison of the CV curves shows that while Mn-PBA displays sharp peaks indicative of abrupt phase transitions, Mn-HEPBA exhibits broader and more gradual redox features[41]. This suggests that the high-entropy effect effectively suppresses localized physical stress and Jahn-Teller distortion at specific potentials. This led to enhanced structural reversibility. The gradual increase in capacity during the initial cycles observed in the GCD profiles represents a structural activation and adaptation process following the initial manganese-ion intercalation.

Moreover, Mn-HEPBA demonstrates outstanding rate capability and capacity recovery even under significant current density variations ranging from 0.1 A g^{-1} to 5.0 A g^{-1}[41]. These results indicate that high-entropy engineering not only stabilizes the framework but also improves ion diffusion pathways while

suppressing transition-metal dissolution. Overall, high-entropy metal-organic frameworks represent a promising platform for overcoming key performance limitations of aqueous manganese-ion batteries and provide an important research direction for the development of high-performance energy storage materials.

In addition, Prussian Blue structures are known to contain a considerable number of intrinsic defects, such as vacancies in the $[Fe(CN)_6]$ framework[41]. The concentration of these defects can significantly influence electrochemical performance by affecting ion transport pathways and structural stability. Therefore, precise control over defect density and distribution will be an important strategy for optimizing the electrochemical properties of Prussian Blue-based electrodes in future manganese-ion battery systems.

CARBON-BASED ANION INTERCALATION MATERIALS (GRAPHITE)

Beyond the conventional single-ion intercalation/de-intercalation mechanisms, dual-ion battery (DIB) systems, which utilize both cations and anions simultaneously, emerge as a transformative alternative to overcome the limited operating voltages of traditional ion batteries. During charging, anions from the electrolyte are intercalated into the cathode, whereas cations are electrochemically deposited/plated onto the anode surface, leading to a progressive decrease in the electrolyte concentration. Conversely, during discharge, the ions stored at each electrode are released back into the electrolyte, facilitating electron flow through the external circuit to generate electricity. This mechanism allows the electrolyte in a DIB system to function not merely as an ion-conductive medium but as an active material directly involved in energy storage.

Notably, this system employs graphite as the cathode; its flexible layered structure provides an interstitial lattice spacing to accommodate anions, which are typically larger than cations. The intercalation of anions into the graphite layers at high potentials significantly enhances the overall operating voltage of the battery. According to research by Cheng *et al.*[14], a high median discharge voltage of approximately 2.34 V was achieved at a charge cut-off of 3.5 V, while maintaining stability over 1,000 cycles. These results demonstrate a performance that significantly surpasses the voltage ranges of conventional aqueous manganese- and zinc-ion batteries.

Figure 7A illustrates the operating mechanism of this manganese dual-ion battery (MDIB), which simultaneously utilizes both cations and anions from the electrolyte for energy storage[14]. The configuration consists of a graphite cathode and a Mn metal anode, utilizing a hybrid organic electrolyte based on $LiPF_6$ and $Mn(TFSI)_2$. Upon charging, Mn^{2+} ions from the electrolyte are deposited onto the anode surface, while PF^{6-} and $TFSI^-$ anions are intercalated into the graphite layers. During discharge, the stored ions undergo de-intercalation/stripping back into the electrolyte to produce electrical energy. Electrochemical performance evaluations via GCD measurements across various voltage windows [Figure 7B] revealed specific capacities of 43.5, 70.3, and 98.6 mAh/g at cut-off voltages of 3.0, 3.3, and 3.5 V, respectively. The corresponding median discharge voltages (V_m) were identified as 2.11, 2.18, and 2.34 V. However, as shown in Figure 7C and D, a degradation in performance was observed during long-term cycling at the higher charge potential of 3.5 V. This is attributed to repeated anion intercalation/de-intercalation at high voltages, which induces cumulative structural strain on the graphite lattice and gradually reduces the reversible ion-storage sites[14].

Nevertheless, Figure 7E confirms that the operating voltage of the MDIB is superior to that of most previously reported zinc-ion batteries. Furthermore, Figure 7F highlights that the MDIB possesses the highest discharge voltage and cycling stability among Mn-ion battery technologies reported to date.

Consequently, if the degradation mechanisms associated with high-voltage operation can be effectively mitigated, this system could become a highly competitive next-generation energy storage solution for grid-scale applications. Importantly, this study highlights the possibility of utilizing anion intercalation to provide

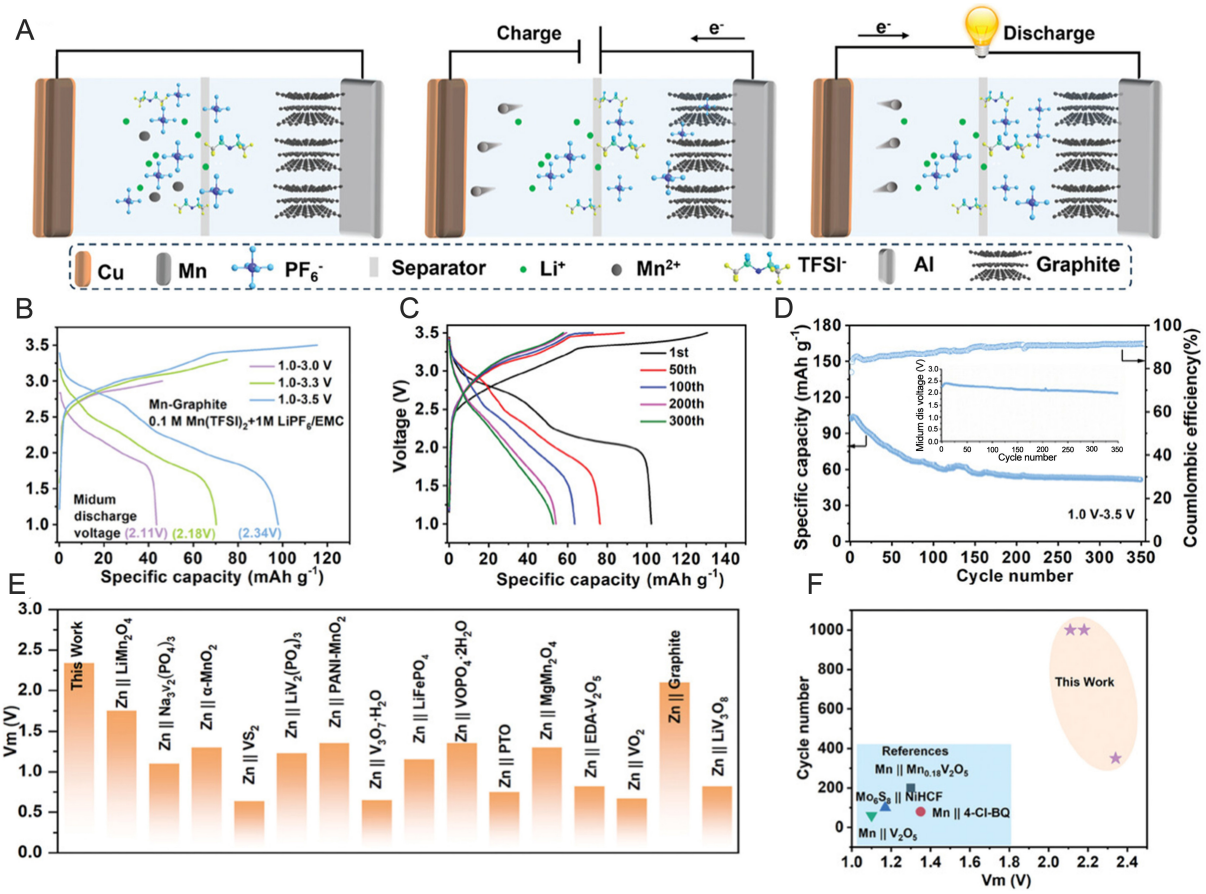

Figure 7. (A) Schematic representation of the MDIB architecture and its dual-ion storage mechanism, utilizing Mn and graphite electrodes within a hybrid $LiPF_6$ and $Mn(TFSI)_2$ electrolyte; (B) Typical GCD profiles recorded across various voltage windows to determine the optimal operational range; (C) Selected GCD curves obtained at specific cycle intervals within the 1.0-3.5 V range; (D) Long-term cycling performance and the corresponding median discharge voltage monitored at 1.0-3.5 V. (E) Comparative analysis of median discharge voltages (V_m) between the present MDIB and previously reported Zn-ion battery systems; (F) Evaluation of cycling stability and discharge voltage in comparison with reported data for various Mn-ion battery technologies. Reprinted with permission from Ref.[14]. Copyright © 2024 Wiley. GCD: Galvanostatic charge-discharge; MDIB: manganese dual-ion battery.

additional charge storage, thereby expanding the accessible capacity beyond conventional cation-based mechanisms. Such behavior represents one of the distinctive features that can be exploited in organic electrode systems.

From a design perspective, enabling simultaneous storage of cations and anions could significantly broaden the operating voltage window while improving overall capacity. Because anions typically possess relatively large ionic sizes, their intercalation generally occurs in layered structures rather than in densely polymerized frameworks, and often involves interactions with the π-electron systems of aromatic rings. Therefore, emphasizing the role of π-electron interactions in ion storage and designing new organic electrode materials that can effectively accommodate both cations and anions may represent a promising strategy for developing high-performance energy storage systems.

CONCLUSION AND OUTLOOK

This review has systematically elucidated the recent technological breakthroughs and strategic design principles for manganese-ion batteries, which are emerging as a pivotal candidate in the next-generation secondary battery market. Figure 8 illustrates the electrochemical performance of the cathode materials discussed in this review. Organic compounds, with the exception of graphite, exhibit relatively high

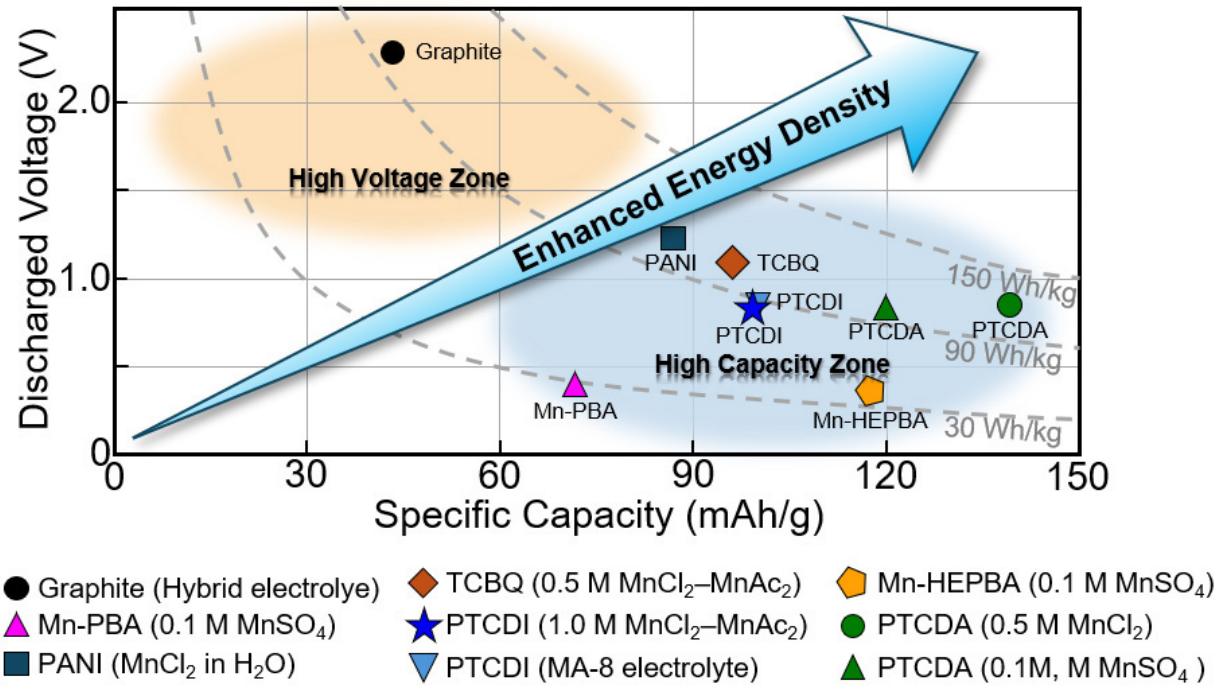

Figure 8. Electrochemical performance comparison of various organic cathode materials for manganese-ion batteries. TCBQ: Tetrachloro-1,4-benzoquinone; PTCDI: perylene-3,4,9,10-tetracarboxylic diimide; PTCDA: perylene-3,4,9,10-tetracarboxylic dianhydride; PANI: polyaniline; PBA: prussian blue analog; HEPBA: high-entropy PBA.

discharge capacities ranging from 70 to over 140 mAh/g, whereas graphite-based materials achieve an elevated discharge voltage surpassing 2.0 V. Traditionally, the commercialization of MIBs has been hindered by the severe structural degradation of inorganic cathodes, primarily due to the strong electrostatic interactions of Mn^{2+} ions and the associated Jahn-Teller distortion. However, recent research has successfully circumvented these chronic limitations by employing innovative platforms such as OCMs, open-framework structures, and dual-ion mechanisms. To provide a clear quantitative overview, Table 1 systematically summarizes the electrochemical metrics, including specific capacity, operating voltage, and energy/power densities for these diverse candidates.

Conjugated carbonyl compounds (e.g., PTCDA and PTCDI) and quinone derivatives (e.g., TCBQ) exhibit excellent reversibility by providing low-strain reaction pathways that accommodate mechanical stress during multivalent ion insertion. Furthermore, conductive polymers like PANI and Prussian Blue analogs have maintained stable power output even under rapid charge-discharge conditions, thanks to their porous and open-framework architectures that offer expansive ion-diffusion channels. Notably, the high-entropy stabilization strategy has been identified as a significant driver for enhancing long-term cycling stability by effectively dispersing localized stresses within complex lattices. Finally, dual-ion battery systems utilizing graphite cathodes have surpassed the voltage limitations of conventional aqueous manganese and zinc batteries, suggesting that MIBs are a formidable candidate to supplement or replace lithium-ion batteries in grid-scale energy storage systems.

Despite these meaningful experimental outcomes, fundamental technical bottlenecks must be addressed through in-depth research to transition MIBs from laboratory-scale experiments to practical, large-scale ESS applications. In particular, a clear distinction must be established between the electrochemical degradation mechanisms of organic and inorganic cathodes to guide targeted optimization. Conventional inorganic frameworks predominantly suffer from severe structural collapse induced by strong electrostatic repulsions,

Table 1. Comparative summary of the electrochemical characteristics for diverse electrode candidates in manganese-based systems

Material	Electrolyte	Counter electrode	Specific capacity (mAh/g)	Average discharge voltage (V *vs.* Mn/Mn^{2+})	Energy density (Wh/kg)	Power density (W/kg)	Reference
PTCDA	Sat. $MnCl_2$ in H_2O	Activated carbon	176	0.83	116.2	1,328	[26]
PTCDA	0.1 M $MnSO_4$ in H_2O	Mn-HEPBA	120	≈0.85	102.0	85	[25]
PTCDI	1.0 M $MnCl_2$ - $MnAc_2$ (Mn^{2+}/Ac^- = 1:1)	Activated carbon	100	≈0.86	86.0	430	[29]
PTCDI	MA-8 Electrolyte ($Mn(ClO_4)_2{\cdot}6H_2O$ + Ac etamide)	Pt electrode	100.5	≈0.86	86.4	4,300	[27]
TCBQ	0.5 M $MnCl_2$-$MnAc_2$	PTCDI	98	1.1	107.8	1,100	[29]
PANI	Sat. $MnCl_2$ in H_2O	Mn metal	88.3	1.27	112.1	317.5	[30]
Mn-HEPBA	0.1 M $MnSO_4$	Activated carbon	117.9	≈0.4	47.2	40	[41]
Mn-PBA	0.1 M $MnSO_4$	Activated carbon	71.8	≈0.38	27.3	38	[41]
Graphite	Hybrid electrolyte of $Mn(TFSI)_2$ and $LiPF_6$	Mn metal	≈43	2.34	100.6	187.2	[14]

PTCDI: Perylene-3,4,9,10-tetracarboxylic diimide; PTCDA: perylene-3,4,9,10-tetracarboxylic dianhydride; TCBQ: tetrachloro-1,4-benzoquinone; PANI: polyaniline; PBA: prussian blue analog; HEPBA: high-entropy PBA.

which is often accompanied by detrimental side reactions and the irreversible formation of insulating $Mn(OH)_2$ on the electrode surface. In sharp contrast, organic counterparts experience an entirely different degradation pathway, where the progressive dissolution of active materials into the aqueous electrolyte represents the primary failure mode. To address this chronic leaching challenge, implementing polymerization strategies has emerged as a highly effective approach, as extending the molecular architecture into polymer chains significantly suppresses solubility in the electrolyte and reinforces long-term cycling stability while preserving structural flexibility.

Addressing active material dissolution and interfacial resistance

While organic cathodes such as PTCDA, PTCDI, and TCBQ offer superior structural flexibility that alleviates mechanical stress during Mn^{2+} insertion, they still suffer from progressive dissolution in aqueous electrolytes. As shown in Figure 4D, the significant difference in cycling stability depending on electrolyte compositions (e.g., with or without acetamide) highlights the critical role of electrolyte environments in stabilizing organic electrodes. In addition, as observed in the Nyquist plot in Figure 6E, the charge-transfer resistance of PANI electrodes increases after long-term cycling, suggesting degradation of ion-transport pathways and interfacial stability. Addressing these challenges will require advanced electrolyte engineering strategies, such as eutectic electrolyte systems and interfacial stabilization approaches, to suppress active material dissolution and maintain stable electrode-electrolyte interfaces. From a materials design perspective, molecular engineering of organic cathodes, such as tuning functional groups, molecular weight, and π-conjugated frameworks, will also be crucial for enhancing structural stability and electrochemical durability.

Structural optimization for multivalent ion accommodation

Open-framework materials such as Prussian Blue analogs enable efficient Mn^{2+} diffusion through their large ion channels; however, localized phase transitions and internal stresses within the framework can still hinder complete reversibility during long-term cycling. As demonstrated by high-entropy PBA systems, introducing compositional complexity can effectively distribute lattice strain and improve structural stability. Therefore, precise control of lattice disorder, defect chemistry, and compositional entropy will be important strategies for optimizing multivalent ion accommodation and achieving long-life manganese-ion batteries. Furthermore, the synergistic interplay between carbonyl redox reactions and π-π interactions is a key factor governing charge-storage behavior. Therefore, systematic compositional analysis and detailed structure-performance evaluation within this class of materials will be essential for optimizing electrochemical performance.

Mitigating electrode degradation at high voltages

Dual-ion battery systems employing graphite cathodes have demonstrated a record-high median discharge voltage of approximately 2.34 V, exceeding the voltage limitations of conventional aqueous manganese batteries. However, as shown in Figure 7C and D, performance degradation occurs during prolonged cycling at high-voltage windows above 3.5 V. This degradation arises from cumulative structural strain in the graphite lattice caused by repeated anion intercalation and de-intercalation at elevated potentials. Future research should therefore focus on designing more robust layered carbon hosts and electrolyte systems capable of stabilizing high-voltage operation. In particular, dual-ion storage chemistry that simultaneously utilizes both cation and anion storage mechanisms represents a promising pathway for achieving wider voltage windows and higher energy density.

Enhancing reversibility and controlling side reactions of Mn metal anodes

Although manganese metal is an attractive anode material due to its low redox potential (-1.19 V *vs.* SHE) and high theoretical capacity, the hydrogen evolution reaction remains a major obstacle to stable cycling. To improve Mn^{2+} plating/stripping reversibility, advanced electrolyte systems such as $Mn(TFSI)_2$ and rational interfacial engineering strategies are required to suppress dendrite formation, corrosion, and parasitic reactions.

Taken together, future progress in manganese-ion batteries will rely on integrated materials design strategies that combine molecular and supramolecular engineering, defect and entropy engineering of open-framework materials, and dual-ion storage chemistry for high-voltage systems. Such synergistic approaches will be essential for overcoming current limitations and enabling safe, high-performance, and sustainable energy storage technologies for grid-scale applications.

In conclusion, the convergence of high-entropy design strategies, structurally flexible organic frameworks, and innovative dual-ion mechanisms will propel Mn-ion batteries to the forefront of safe and cost-effective next-generation ESS solutions. By harmonizing the precise molecular design of cathodes with advanced electrolyte engineering, MIBs are poised to transcend current performance bottlenecks and position manganese-ion batteries as a viable alternative for safe and sustainable grid-scale energy storage.

DECLARATIONS

Authors' contributions

Conceived the manuscript: Lee, H.; Chae, M. S.
Wrote the manuscript: Lee, H.
Reviewed the manuscript: Chae, M. S.
Contributed to the discussion of the manuscript: Chae, M. S.; Yang, J.; Kim, J.; Chae, M. S.

Availability of data and materials

Not applicable.

AI and AI-assisted tools statement

During the preparation of this manuscript, the AI tool ChatGPT (version GPT-5.5, released 2026-04-23) was used solely for language editing. The tool did not influence the study design, data collection, analysis, interpretation, or the scientific content of the work. All authors take full responsibility for the accuracy, integrity, and final content of the manuscript.

Financial support and sponsorship

This work was supported by the Hyundai Motor Chung Mong-Koo Foundation and the National Research Foundation of Korea (NRF) grant funded by the Korean government (MSIT) (RS-2026-25470628).

Conflicts of interest

All authors declared that there are no conflicts of interest.

Ethical approval and consent to participate

Not applicable.

Consent for publication

Not applicable.

REFERENCES

1. Divya, K.; Østergaard, J. Battery energy storage technology for power systems-an overview. *Electr. Power. Syst. Res.* **2009**, *79*, 511-20. DOI
2. Li, M.; Lu, J.; Chen, Z.; Amine, K. 30 years of lithium-ion batteries. *Adv. Mater.* **2018**, , e1800561. DOI
3. Kalungi, P.; Yao, Z.; Huang, H. Aspects of nickel, cobalt and lithium, the three key elements for Li-ion batteries: an overview on resources, demands, and production. *Materials* **2024**, *17*, 4389. DOI PubMed PMC
4. Zhang, L.; Jin, K.; Sun, J.; Wang, Q. A review of fire-extinguishing agents and fire suppression strategies for lithium-ion batteries fire. *Fire. Tech.* **2024**, *60*, 817-58. DOI
5. Bravo, Diaz. L.; He, X.; Hu, Z.; et al. Review-meta-review of fire safety of lithium-ion batteries: industry challenges and research contributions. *J. Electrochem. Soc.* **2020**, *167*, 090559. DOI
6. Liang, Y.; Yao, Y. Designing modern aqueous batteries. *Nat. Rev. Mater.* **2023**, *8*, 109-22. DOI
7. Ahn, H.; Kim, D.; Lee, M.; Nam, K. W. Challenges and possibilities for aqueous battery systems. *Commun. Mater.* **2023**, *4*, 367. DOI
8. Chao, D.; Zhou, W.; Xie, F.; et al. Roadmap for advanced aqueous batteries: from design of materials to applications. *Sci. Adv.* **2020**, *6*, eaba4098. DOI PubMed PMC
9. Li, H.; Zhang, W.; Sun, K.; et al. Manganese-based materials for rechargeable batteries beyond lithium-ion. *Adv. Energy. Mater.* **2021**, *11*, 2100867. DOI
10. Luo, H.; Su, X.; Chen, Z.; et al. Aqueous iron-ions batteries: status, solutions, and prospects. *Adv. Mater.* **2025**, *37*, e2507978. DOI
11. Bi, S.; Wang, S.; Yue, F.; Tie, Z.; Niu, Z. A rechargeable aqueous manganese-ion battery based on intercalation chemistry. *Nat. Commun.* **2021**, *12*, 6991. DOI PubMed PMC
12. Wang, M.; Meng, Y.; Xu, Y.; Shen, D.; Tong, P.; Chen, W. An energetic aqueous Mn metal anode. *ACS. Energy. Lett.* **2024**, *9*, 1381-8. DOI
13. Luo, H.; Guo, H.; Li, X.; et al. Aqueous manganese-ion batteries: the past, present, and future. *Matter* **2025**, *8*, 102379. DOI
14. Cheng, Z.; Dong, Q.; Pu, G.; Song, J.; Zhong, W.; Wang, J. A durable and high-voltage Mn-graphite dual-ion battery using Mn-based hybrid electrolytes. *Small* **2024**, *20*, e2400389. DOI
15. Zhang, J.; Chen, F.; Yu, J.; et al. Asymmetric Mn^{2+} cluster electrolyte for high-performance Mn-metal batteries. *Adv. Funct. Materials.* **2026**, *36*, e15536. DOI
16. Zhang, J.; Chen, F.; Liu, Z.; et al. Single halide electrolytes for high-performance Mn metal batteries. *Angew. Chem. Int. Ed.* **2026**, *65*, e25344. DOI
17. Yao, Q.; Fu, Y.; Tian, C.; et al. Co-solvent electrolyte engineering enables reversible and high-energy aqueous manganese metal batteries. *Adv. Funct. Mater.* **2026**, *36*, e23268. DOI

18. Pyun, J.; Lee, H.; Baek, S.; et al. Nonaqueous electrolyte rechargeable manganese batteries with potassium manganese hexacyanoferrate cathodes. *Adv. Sci.* **2025**, *12*, e2500132. DOI PubMed PMC
19. Shen, D.; Zheng, X.; Luo, R.; et al. A rechargeable, non-aqueous manganese metal battery enabled by electrolyte regulation. *Joule* **2024**, *8*, 780-98. DOI
20. Li, M.; Li, C.; Zuo, C.; et al. Strategically modulating proton activity and electric double layer adsorption for innovative all-vanadium aqueous Mn^{2+}/proton hybrid batteries. *Adv. Mater.* **2024**, *36*, e2407233. DOI
21. Liu, P.; Zhu, K.; Gao, Y.; Luo, H.; Lu, L. Recent progress in the applications of vanadium-based oxides on energy storage: from low-dimensional nanomaterials synthesis to 3D micro/nano-structures and free-standing electrodes fabrication. *Adv. Energy. Mater.* **2017**, *7*, 1700547. DOI
22. Xu, X.; Wang, T.; Zhao, X.; Qu, X.; Jiao, L.; Liu, Y. Dual-site Mn-doped vanadate cathodes involving vanadium and manganese dual redox chemistry for high-energy aqueous zinc-ion batteries. *ACS. Energy. Lett.* **2025**, *10*, 5057-66. DOI
23. Zhu, X.; Cao, Z.; Li, X.; et al. Ion-intercalation regulation of MXene-derived hydrated vanadates for high-rate and long-life Zn-Ion batteries. *Energy. Storage. Mater.* **2022**, *45*, 568-77. DOI
24. Miao, L.; Song, Z.; Du, W.; et al. Advances in organic cathode materials for aqueous multivalent metal-ion storage. *Mater. Chem. Front.* **2023**, *7*, 2731-49. DOI
25. Dong, S.; Xu, Z.; Cao, Z.; et al. Aqueous "rocking-chair" Mn-ion battery based on an industrial pigment anode. *Chem. Eng. J.* **2024**, *501*, 157774. DOI
26. Lee, H.; Nimkar, A.; Shpigel, N.; et al. π-electron-assisted charge storage in fused-ring aromatic carbonyl electrodes for aqueous manganese-ion batteries. *ACS. Energy. Lett.* **2024**, *9*, 5627-34. DOI
27. Dai, T.; Yang, B.; Wei, J.; et al. Environmentally benign and long cycling Mn-ion full batteries enabled by hydrated eutectic electrolytes and polycarbonyl conjugated organic anodes. *J. Am. Chem. Soc.* **2025**, *147*, 13721-31. DOI
28. He, X.; Li, Z.; Tang, R.; et al. Rechargeable and highly stable Mn metal batteries based on organic electrolyte. *Chem. Commun.* **2023**, *59*, 1337-40. DOI
29. Cai, L.; Zhang, Y.; Yuan, W.; et al. Ion-specific acetate-Mn^{2+} coordination for accelerating desolvation kinetics in aqueous Mn-ion battery. *Adv. Energy. Mater.* **2025**, *15*, 2501026. DOI
30. Lee, H.; Pyun, J.; Kwon, H.; Chae, M. S. High-voltage aqueous manganese-ion batteries enabled by a semi-crystalline polyaniline cathode and Mn metal anode. *Small* **2026**, *22*, e14020. DOI PubMed
31. Salah, M.; Qasim, K. F.; Shama, S. A.; Mousa, M. A. Influence of Co-Mn mutual co-insertion in physicochemical properties of vanadate compounds for energy storage systems. *J. Power. Sources.* **2025**, *652*, 237545. DOI
32. Soundharrajan, V.; Nithiananth, S.; Lee, J.; et al. Manganese ion batteries: LiV_3O_8 nanorods as a robust and long-life cathode module. *J. Power. Sources.* **2023**, *558*, 232542. DOI
33. Soundharrajan, V.; Lee, J.; Kim, S.; Kim, J. H.; Hwang, J.; Kim, J. An aqueous manganese-ion battery with NaV_6O_{15}/C microrods as a stable Mn^{2+} storage host. *Batteries. Supercaps.* **2023**, *6*, e202200527. DOI
34. Lu, C.; Chen, X.; Hu, Y.; et al. A dual-carbon engineering strategy enabled high-activity hierarchical manganese vanadate cathode for long-cycling aqueous zinc-ion batteries. *Electrochimica. Acta.* **2026**, *555*, 148393. DOI
35. Liebl, S.; Gallmetzer, J. M.; Werner, D.; Apaydin, D. H.; Hofer, T. S.; Portenkirchner, E. Perylenetetracarboxylic diimide composite electrodes as organic cathode materials for rechargeable sodium-ion batteries: a joint experimental and theoretical study. *ACS. Omega.* **2024**, *9*, 6642-57. DOI PubMed PMC
36. Yang, X.; Ni, Y.; Lu, Y.; et al. Designing quinone-based anodes with rapid kinetics for rechargeable proton batteries. *Angew. Chem. Int. Ed.* **2022**, *61*, e202209642. DOI
37. Bi, S.; Zhang, Y.; Deng, S.; Tie, Z.; Niu, Z. Proton-assisted aqueous manganese-ion battery chemistry. *Angew. Chem. Int. Ed.* **2022**, *61*, e202200809. DOI PubMed
38. Yang, Y.; Zhou, J.; Wang, L.; et al. Prussian blue and its analogues as cathode materials for Na-, K-, Mg-, Ca-, Zn- and Al-ion batteries. *Nano. Energy.* **2022**, *99*, 107424. DOI
39. Jiang, L.; Lu, Y.; Zhao, C.; et al. Building aqueous K-ion batteries for energy storage. *Nat. Energy.* **2019**, *4*, 495-503. DOI
40. He, Y.; Dreyer, S. L.; Akçay, T.; et al. Leveraging entropy and crystal structure engineering in prussian blue analogue cathodes for advancing sodium-ion batteries. *ACS. Nano.* **2024**, *18*, 24441-57. DOI
41. Xu, Z.; Cao, Z.; Yang, Y.; et al. High-entropy engineering of Prussian blue analog enables high-stable Mn-ion storage with ion selectivity and structure stability. *Energy. Storage. Mater.* **2025**, *81*, 104457. DOI